

Supplementary Information

Crystal structure and compositional effects on the electrical and electrochemical properties of $\text{GdBaCo}_{2-x}\text{Mn}_x\text{O}_{5+\delta}$ ($0 \leq x \leq 2$) oxides for use as air electrodes in solid oxide fuel cells

Daniel Muñoz-Gil, Esteban Urones-Garrote, Domingo Pérez-Coll, Ulises Amador and Susana García-Martín

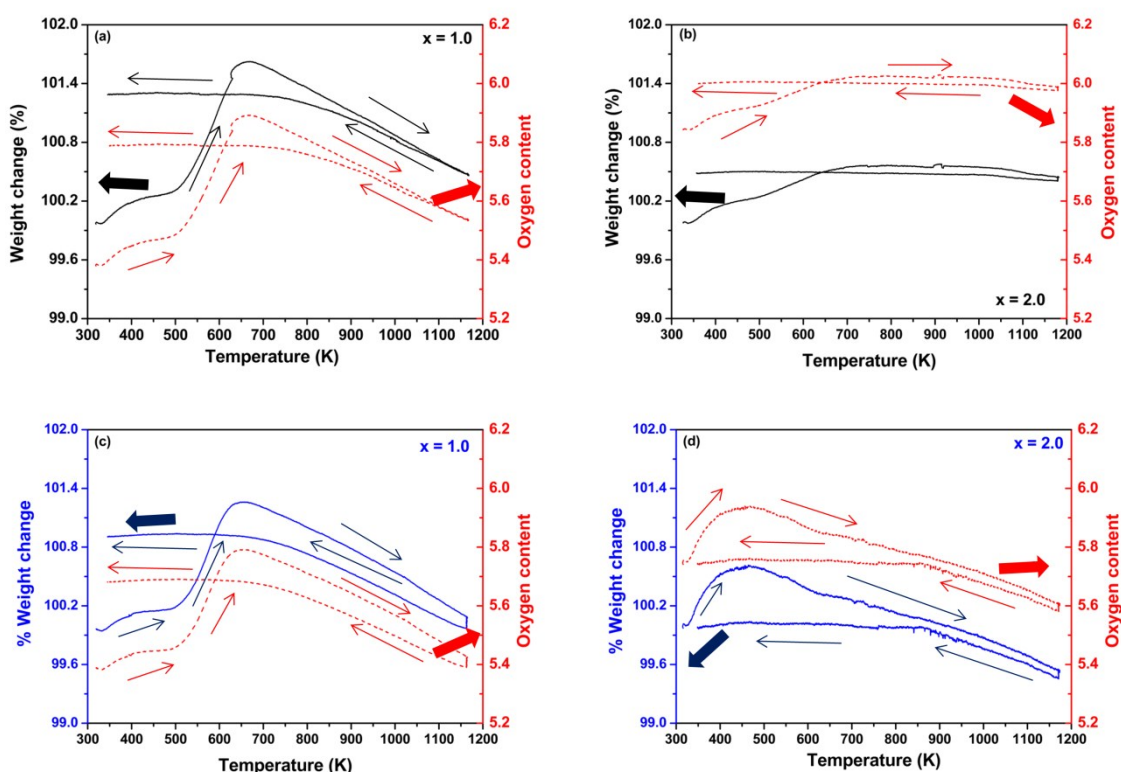


Figure S1. Thermogravimetric curves collected in ambient air, from room temperature to 1173 K, of $\text{GdBaCo}_{2-x}\text{Mn}_x\text{O}_{5+\delta}$ oxides with $x = 1.0$ and 2.0 prepared in: (a, b) air and (c, d) argon. Heating and cooling cycles are indicated by arrows. Initial oxygen content of $\text{GdBaCo}_{2-x}\text{Mn}_x\text{O}_{5+\delta}$ determined from redox titration.

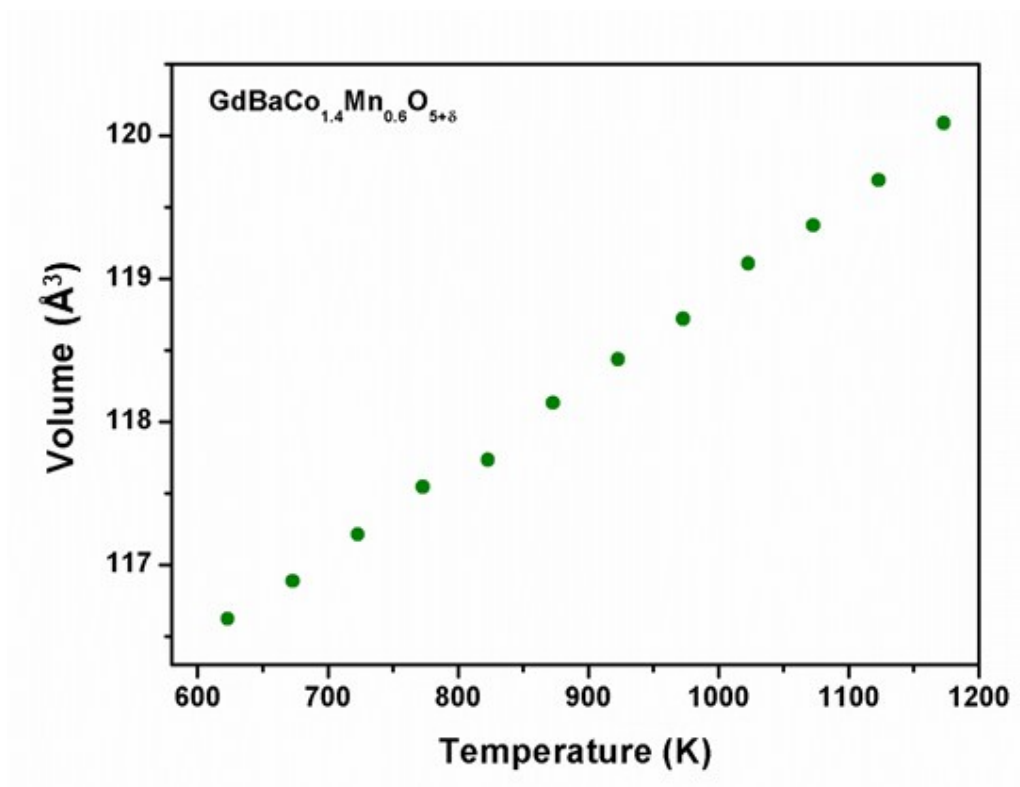


Figure S2. Thermal evolution of the cell volume for $\text{GdBaCo}_{1.4}\text{Mn}_{0.6}\text{O}_{5+\delta}$ prepared in air. All the compounds of the $\text{GdBaCo}_{2-x}\text{Mn}_x\text{O}_{5+\delta}$ system show a similar linear variation of the cell-volume with temperature.

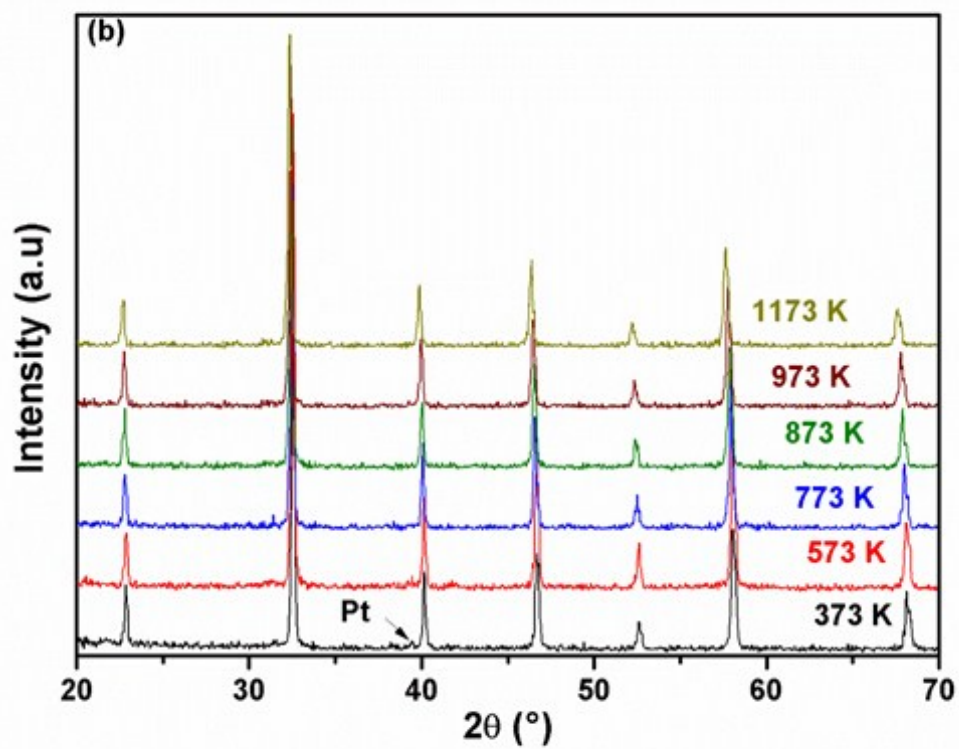
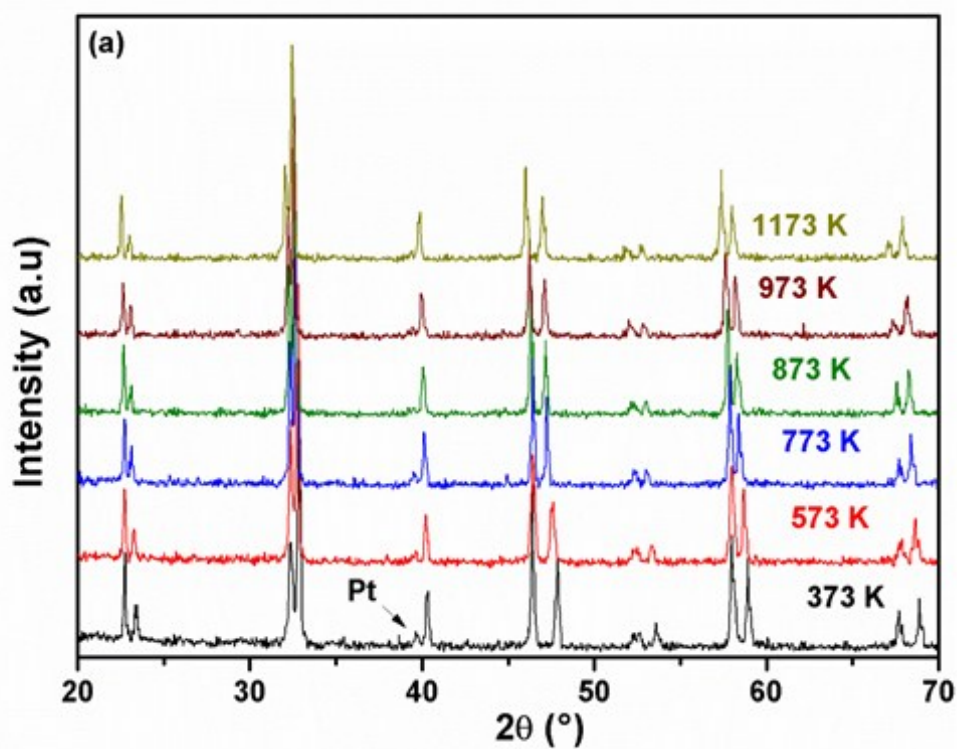


Figure S3. PXRD patterns at different temperatures taken from room temperature to 1173 K of (a) $\text{GdBaCo}_{1.8}\text{Mn}_{0.2}\text{O}_{5+\delta}$, (b) $\text{Gd}_{0.5}\text{Ba}_{0.5}\text{Co}_{0.2}\text{Mn}_{0.8}\text{O}_{3-\delta}$ prepared in air. Reflections associated to the Pt sample holder are sometimes detected in the pattern.

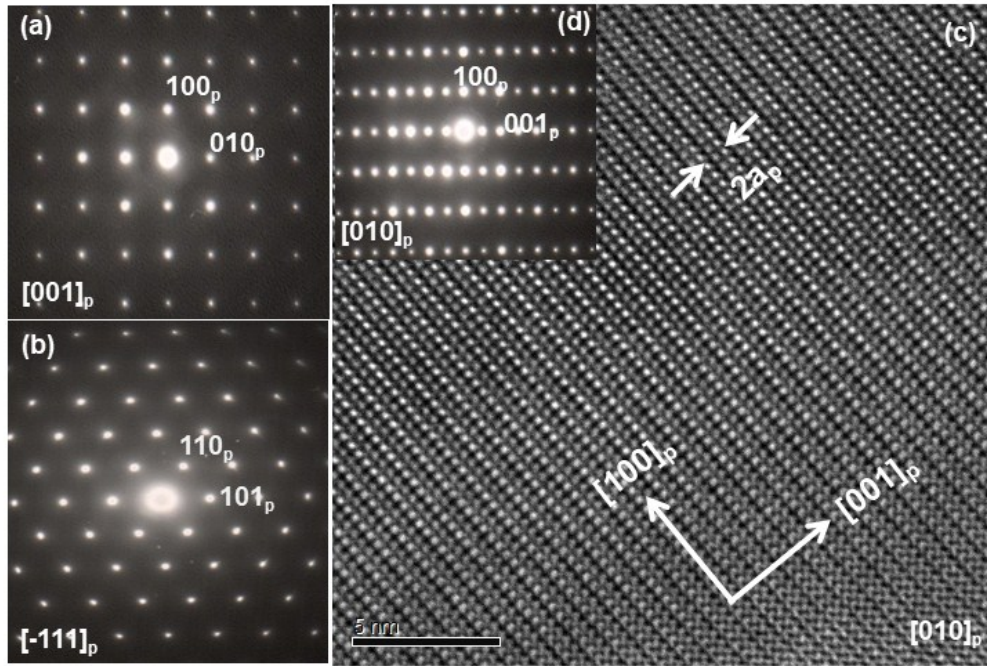


Figure S4a. SAED patterns of a $\text{GdBaCoMnO}_{5+\delta}$ crystal along (a) the $[001]_p$ and (b) $[-111]_p$ zone axes. (c) HRTEM image of a $\text{GdBaCoMnO}_{5+\delta}$ crystal along the $[010]_p$ zone axis and (d) the corresponding SAED pattern. The patterns are indexed according to the cubic perovskite structure. Extra reflections indicate a two-fold modulation of the crystal structure along the $[001]_p$ direction. Contrast differences in the HRTEM image indicate a $2a_p$ periodicity along the $[001]_p$ direction. These results are in agreement with the $a_p \times a_p \times 2a_p$ unit cell associated to layered-type ordering of the cations. All the oxides with layered-type ordering of Gd and Ba of the $\text{GdBaCo}_{2-x}\text{Mn}_x\text{O}_{5+\delta}$ system show similar SAED patterns and HRTEM images.

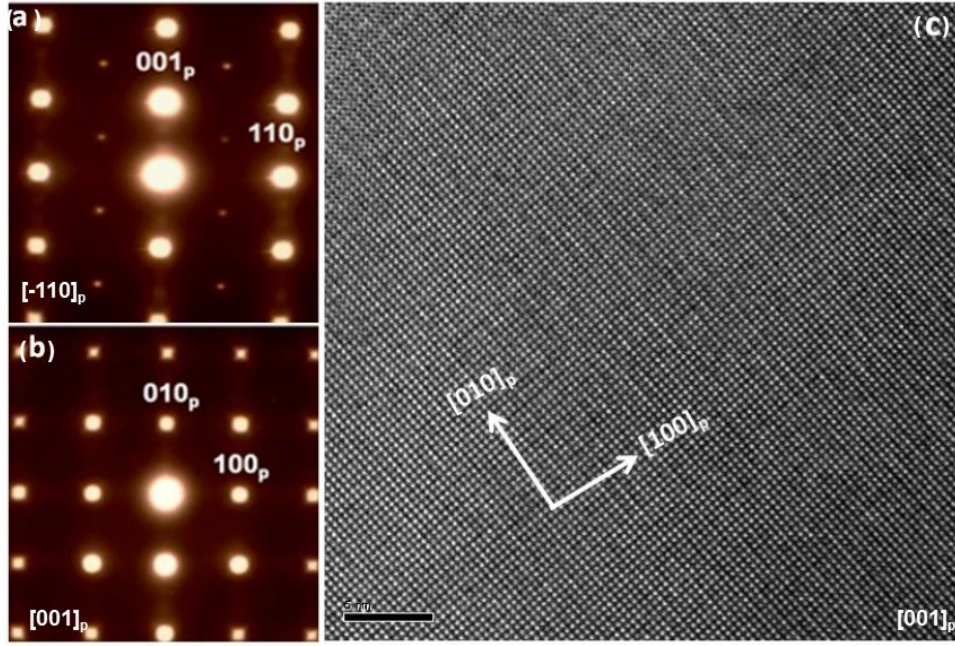


Figure S4b. SAED patterns of a $\text{Gd}_{0.5}\text{Ba}_{0.5}\text{MnO}_{3-\delta}$ crystal along (a) the $[-110]_p$ and (b) $[001]_p$ zone axes. (c) HRTEM image of a $\text{Gd}_{0.5}\text{Ba}_{0.5}\text{MnO}_{3-\delta}$ crystal along the $[001]_p$ zone axis. The patterns are indexed according to the cubic perovskite structure. The contrast differences in the HRTEM image are characteristic of perovskite structure, however weak reflections in the SAED pattern along the $[-110]_p$ zone axis at $G_p \pm 1/2(111)^*_p$ are associated to tilting of the oxygen octahedral network giving a unit cell $\sqrt{2}a_p \times \sqrt{2}a_p \times 2a_p$ unit cell. All the oxides without layered-type ordering of Gd and Ba of the $\text{GdBaCo}_{2-x}\text{Mn}_x\text{O}_{5+\delta}$ system (therefore $\text{Gd}_{0.5}\text{Ba}_{0.5}\text{Co}_{0.5-x}\text{Mn}_x\text{O}_{3-\delta}$) show similar SAED patterns and HRTEM images.

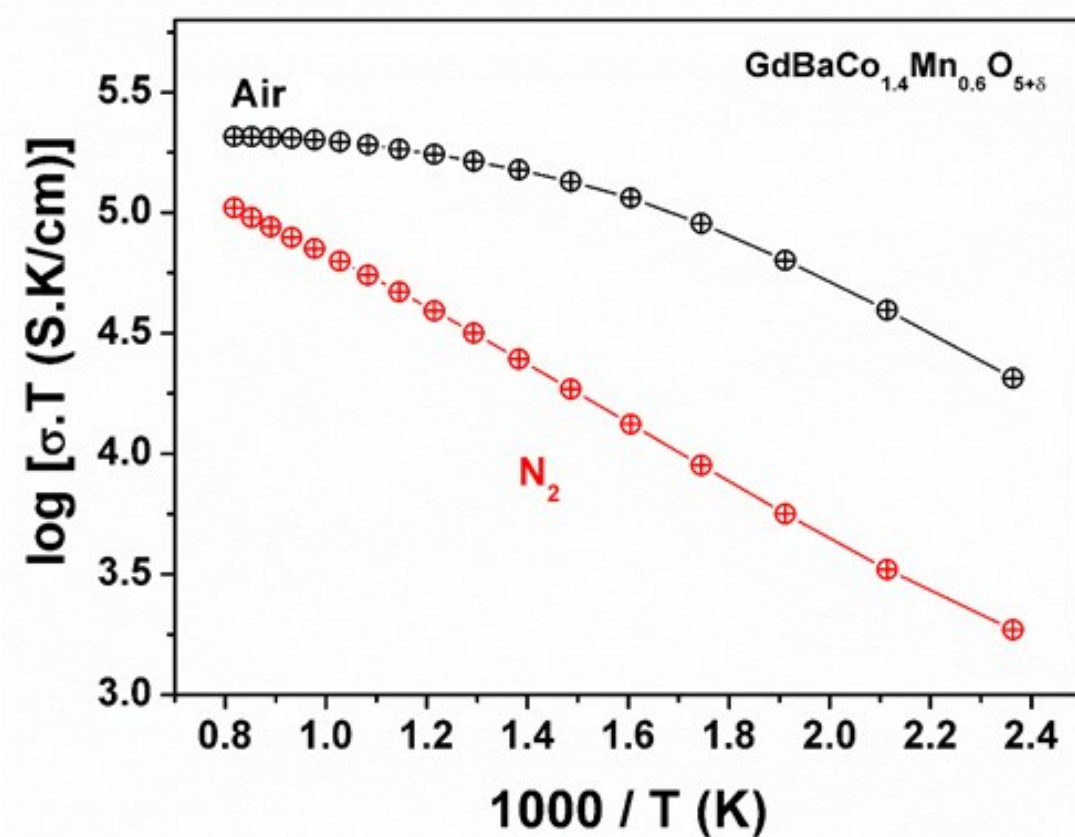


Figure S5. Arrhenius representation of the total conductivity measured in N_2 and air atmospheres of the $\text{GdBaCo}_{1.4}\text{Mn}_{0.6}\text{O}_{5+\delta}$ prepared in argon. The higher values of conductivity obtained for higher oxidizing conditions confirms the electron-hole character of the conduction process. Similar behavior is found in all the oxides of the system.

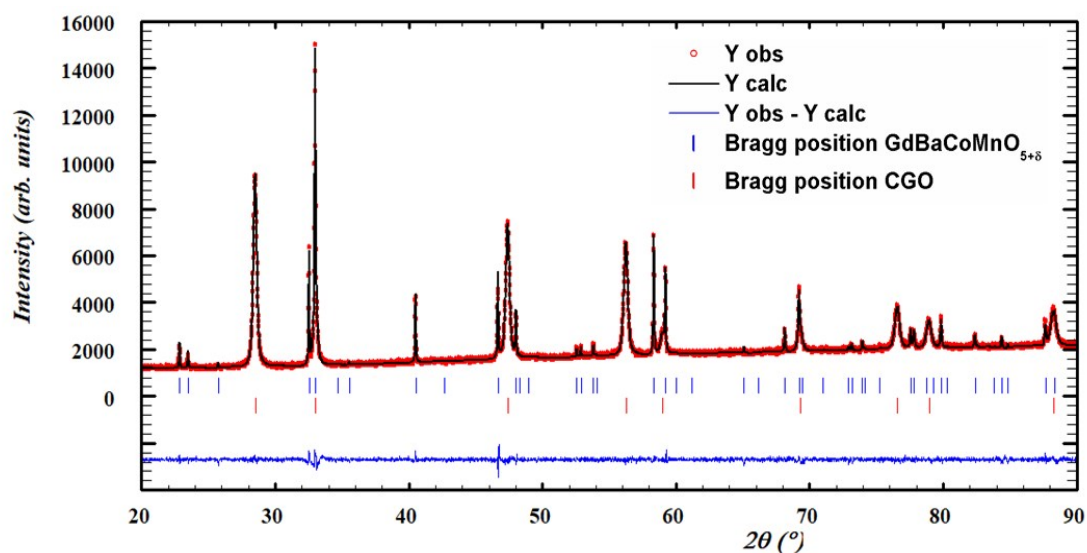


Figure S6. PXRD pattern of the composite $\text{GdBaCoMnO}_{5+\delta}:\text{CGO}$ (70 : 30 wt%) heated at 1173 K for 12 hours. The $\text{GdBaCoMnO}_{5+\delta}$ was prepared in air. All the Bragg positions of the pattern correspond to either $\text{GdBaCoMnO}_{5+\delta}$ or CGO.

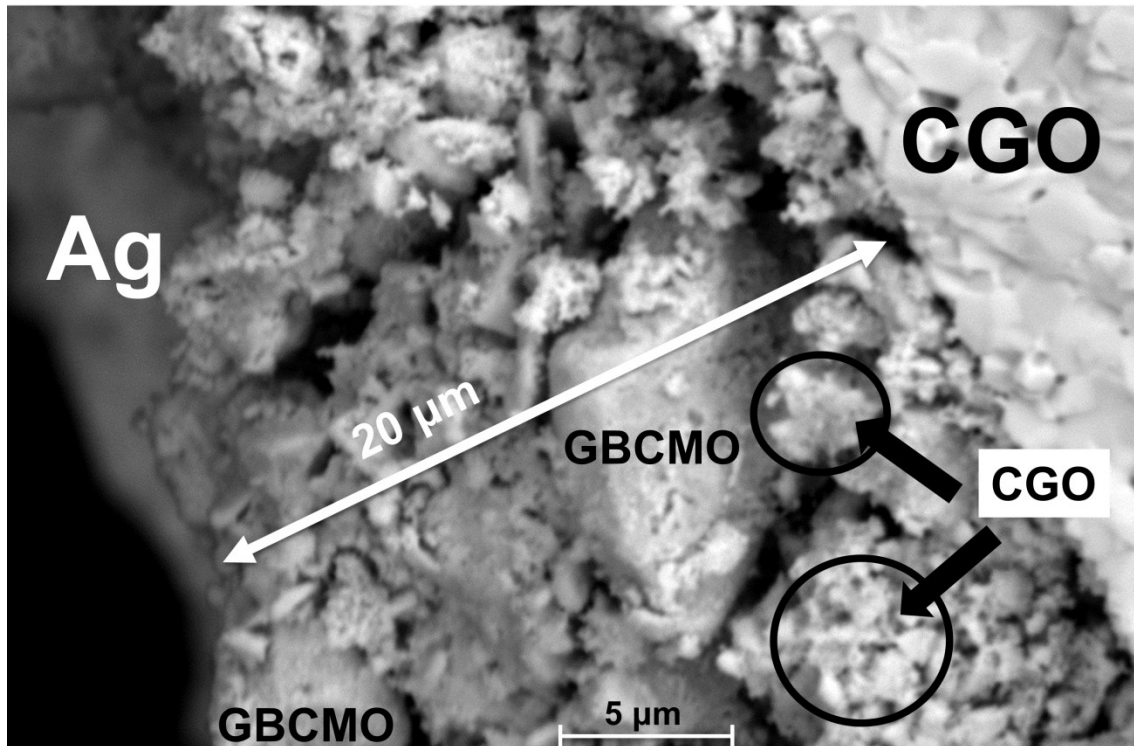


Figure S7. SEM cross-section image of symmetrical cell GBCMO:CGO /CGO/GBCMO:CGO with GBCMO being $\text{GdBaCoMnO}_{5+\delta}$ prepared in air.

Different systems possess minor differences in microstructural parameters such as grain size, open porosity and distribution of ionic and electronic conducting phases, as a consequence of the same procedure followed for the preparation of the symmetrical cells.

